

THE ORNL FAST WAVE ICRF ANTENNA FOR ALCATOR C-MOD

R. H. Goulding, D. J. Hoffman, D. L. Conner, C. J. Hammonds,
J. L. Ping, B. W. Riemer, P. M. Ryan, D. J. Taylor,
R. B. Wysor, J. J. Yugo[†]

Oak Ridge National Laboratory

P. O. Box 2009 Oak Ridge, Tennessee 37831-8071

Abstract

A fast wave ICRF antenna is being designed for Alcator C-Mod which is prototypical in many respects of the baseline launcher design for the Compact Ignition Tokamak (CIT). The C-Mod launcher has a single current strap, with a strap and cavity geometry very similar to one quadrant of the CIT launcher, which has four straps in a 2 x 2 configuration. The antenna fits entirely within an 8 in. wide by 25 in. long port and is radially moveable over a distance of 15 cm. It will operate at a frequency of 80 MHz for pulse lengths up to 1 s, at a maximum power level of 2 MW, corresponding to a power flux of $> 1.5 \text{ kW/cm}^2$. The antenna is an end fed double loop configuration in which the current strap is grounded in the middle to provide mechanical support. The design includes a disruption support system which accommodates thermal expansion of the antenna box while supporting large disruption loads. It also includes a novel matching system consisting of an external resonant loop with two shunt capacitors serving as tuning/ matching elements.

Introduction

A high power density fast-wave Ion Cyclotron Range of Frequencies (ICRF) antenna is being designed at ORNL, which will incorporate many features relevant to operation in next generation tokamak experiments. The antenna will be installed and operated in the Alcator C-Mod Tokamak, and is specifically designed to be prototypical in as many aspects as possible of the launcher currently proposed for use on the Compact Ignition Tokamak (CIT)¹. The antenna will operate at power levels up to 2 MW, for pulse lengths up to 1 s, at a frequency of 80 MHz, which corresponds to $\Omega_{3\text{He}}$ at 7.9 T. The antenna is a single strap, end fed configuration with the strap grounded at the center.

There are several notable features of the design that make it well suited to application in next generation tokamaks. It features a disruption support system able to withstand loads generated by a 3 MA /3 ms disruption at 9 T, while allowing considerable thermal expansion of the antenna box relative to the port that it is located in, or conversely, contraction of the port. The design of the disruption support structure allows installation or removal of the entire launcher including supports from outside the port, greatly simplifying remote maintenance.

The Faraday shield elements, which are cylindrical Inconel rods, are designed to have very low primary thermal stresses, facilitating the handling of high power densities. In the CIT Faraday shield these solid Inconel rods can be replaced by tubes, allowing direct liquid cooling of shield elements without changing the electrical characteristics of the shield design.

Ceramic feedthroughs are located outside the vacuum vessel, where exposure to ionizing radiation, which may enhance rf losses and seriously

[†]Fusion Engineering Design Center, Oak Ridge National Laboratory, Oak Ridge, TN

* Research sponsored by the Office of Fusion Energy, U.S. Department of Energy, under Contract DE-AC05-84OR21400 with Martin Marietta Energy Systems, Inc.

MASTER

DISTRIBUTION OF THIS DOCUMENT IS UNLIMITED

degrade the feedthrough life expectancy², can be limited. There are no ceramic supports between the current strap and these feedthroughs.

The antenna is tuned and matched using an external resonant loop employing integral capacitors to achieve a match at the loop feed point. This system is capable of meeting the 2MW / strap power requirement while being compact enough so that the entire matching system can fit within the CIT shield wall, eliminating spurious resonances and power handling difficulties caused by long unmatched transmission line runs. It also allows tuning in 2-3 frequency bands without modifying the physical layout of the system¹.

Mechanical Design

General Description

Figure 1. is a side view of the launcher. The current strap, antenna backplane, antenna cavity, and Faraday shield components are all fabricated from Inconel in order to withstand forces generated by disruptions. Molybdenum bumpers are provided to protect the side walls of the antenna. Current carrying surfaces are all plated with copper or silver. The current strap is 8 cm wide and 48 cm in total length. It is grounded at the center through a support that is bolted to the antenna backplane. The minimum distance from the back of the current strap to the backplane is 8.8 cm. The antenna cavity is 13.3 cm wide and has solid sidewalls extending from the backplane to within 1 cm of the back of the current strap.

There are a total of 56 Faraday shield elements consisting of cylindrical Inconel rods bent into a flattened U shape (Fig 2.) and arranged in two tiers. The front rods are 1.27 cm in diameter while the rear rods are 0.95 cm in diameter. The rods in the front tier are ground flat at the front, reducing the total shield thickness. All rods are plated with copper and then coated with a layer of titanium carbonitride approximately 7 μm thick. The rods are welded into a support frame which is bolted to the antenna box sidewalls.

The antenna is supported at the front by the disruption support system, which is described in more detail below. Additional support is provided by rollers attached to flanges in the resonant loop coaxial line, as shown in Figure 1. Radial loads resulting from disruptions and vacuum loads are carried by a support yoke which is connected by an electric motor driven actuator to the port cover plate, allowing radial translation of the antenna.

Power is fed to ends of the straps by two coaxial $50\ \Omega$ copper plated stainless steel transmission lines. The outer conductors have an outer diameter of 140 mm and a wall thickness of 6 mm. There are bellows in the center conductor lines between the current strap and the vacuum feedthroughs to allow thermal expansion of the center conductors relative to the outer conductor and to reduce transmission of disruption loads from the current strap to the ceramic feedthroughs. The primary vacuum feedthroughs for the antenna are located 1.7 m from the current strap ends. The design of these feedthroughs has been described elsewhere³. The balance of the resonant circuit beyond the feedthroughs is fabricated from standard 9 in. (230 mm) $50\ \Omega$ copper transmission line. There is a secondary vacuum feedthrough beyond the resonant loop feed point (Fig. 1), allowing this section of line to be operated under high (10^{-7} Torr) vacuum, separate from the machine vacuum. This is done to allow operation with a high voltage standing wave ratio (VSWR) without requiring pressurization with SF₆, which is not acceptable for use on CIT. A 2 in. pump out port is provided between this feedthrough and the tee. The flanges on the

transmission line will be modified if necessary to achieve the required vacuum.

Disruption Support Mechanism

The disruption support mechanism is designed to allow the entire antenna including disruption supports to be installed from outside the vacuum vessel, considerably simplifying remote handling in a CIT type of environment. It is designed to carry transverse loads only, which are predicted to be much larger than radial loads, according to force calculations performed for a similar ICRF antenna designed by MIT for use in Alcator C-Mod⁴. Elimination of gaps between contacting surfaces allows large loads to be carried, but the design also allows for thermal expansion of the antenna box relative to the port in which it is supported.

The present design for the support mechanism (fig. 3) calls for two identical assemblies located at the top and bottom of the antenna box. Each assembly includes a semi-cylindrical wedge swivel (or key) fitting into a wedge way running along the top or bottom of the antenna box, and a bearing/wedge housing supporting bearing pads which contact the vacuum vessel port wall at the joint between the vacuum vessel and the port nozzle. Loads are transmitted to the housing through two adjustable wedges in the form of truncated hexagonal pyramids. The shape was chosen to allow surface contact as the wedges are moved in and out. The pyramids are tapered at an angle of 8°, which is 2.5 to 4 times the self locking angle, so that the wedges will move apart in response to thermal contraction of the port (or expansion of the antenna frame).

The wedges in the bottom assembly are adjusted by means of a nut, which in the C-Mod design cannot be adjusted remotely. The force on the top wedges is applied through a 2 in. ID hydraulic cylinder, with the outer wedge connected to the piston by a rod, and the inner wedge connected to the cylinder by a concentric sleeve. Pressure can be applied to either side of the piston, serving either to force the wedges towards each other and pre-load the bearing pads during normal operation, or to break the wedges free should it become necessary in order to permit radial movement of the antenna. The key and beam are held in a fixed position relative to the port by a cylindrical support extending back to the port cover plate.

All sliding surfaces are coated with a 1 μ m thick layer of tungsten disulfide which is diffusion bonded to the metal surfaces. This coating serves as a lubricant and prevents vacuum welding. It is particularly well suited for this application in that it has a low friction coefficient (.025 - .065), a high load capacity, a wide range of operating temperatures, and a very low vapor pressure after bonding.

During operation, a constant force is applied to the piston, so that the support mechanism self-adjusts for relative thermal expansion of the antenna frame. The response time of the system is slow compared to the time scale of a disruption, so that in this case the full loads are transmitted through the wedges to the vacuum vessel.

Antenna Cooling

An extensive analysis of antenna heating due to both rf and plasma sources is currently underway. Preliminary results indicate that Faraday shield tubes can be held to safe temperatures (~ 600° C maximum) for the specified pulse duration (1 s rf, 3 s plasma every 20 m) if the backplane is maintained at a fixed 30° C temperature by active cooling. A system for trace cooling of the back side of the back plane has been incorporated into the design, but the cooling medium has not yet been decided upon. Further work is currently underway to

better model the power deposition profiles on the Faraday shield, and to determine the cooling requirements necessary to achieve a considerably higher rf duty cycle during antenna conditioning.

Electrical Design

Antenna/Cavity

The current strap is an end fed double loop design which is grounded at the center. We have examined means of optimizing the current strap, Faraday shield, and cavity geometry in order to maximize the power handling capability of the antenna.

Power Handling Optimization One optimization parameter that has been examined is the ratio of the peak rf power dissipation to the value averaged over the region in which the power dissipation is non-negligible. This parameter determines in part the peak temperature reached on the shield after a pulse. This quantity was determined for a range of current strap widths by calculating the rf magnetic field amplitudes at the surface of the shield elements (without the elements present) using a 2-D magnetostatic code⁵ which includes the effects of the current strap and cavity geometry. The effect of the shield elements on the field is primarily to increase the amplitude of the field components normal to the axis of the rods in the gaps between them, and was included using results of an analogous 2-D electrostatic calculation, as described in Ref. 6. Results of the calculation have shown that varying the current strap width has little effect on the ratio of peak to average power dissipation levels (as defined above), and serves only to change the locations of the peak dissipation regions.

Other optimization strategies that were considered were the minimization of the peak voltages on the current strap and the tuning loop for a given value of coupled power. The peak voltage on the current strap for a given power level is proportional to $L / R^{1/2}$ where L is the inductance per unit length of the strap and R is the resistance (including radiation resistance) per unit length. The peak voltage in the resonant loop is proportional to the square root of the VSWR in the lines between the current strap and the tuning capacitors.

Transmission line analysis The 2-D magnetostatic code referenced previously was used to determine transmission line parameters for the current strap for use in a transmission line analysis. Values of L and relative values of R for different strap widths and different slot lengths in the sidewalls were obtained. The absolute magnitude of R depends on the plasma surface impedance, which is not modeled in the code. The code treats the plasma as a perfectly conducting surface. Relative changes in R due to changes in antenna geometry are accurately modeled by the code, as was demonstrated in low power loading measurements performed on the DIII-D tokamak⁷. The strap capacitance per unit length is not calculated in the code, but was assumed to remain constant as the slot length is changed. This is a reasonable assumption since the capacitance is expected to change very little if the slotted side wall is replaced by a continuous wall. On the other hand, as the strap width is varied the capacitance changes with the change in surface area. In this case it was assumed that the phase velocity remains constant.

Using the assumptions stated above, and an arbitrary value of .54 for the phase velocity for the case in which the side slots extend 1 cm behind the current strap (based on measurements from a different antenna), a transmission line analysis was used to determine the maximum strap and resonant loop voltages as a function of strap width and slot length. The absolute magnitude of

the resistive loading was taken to be a conservative value of $8 \Omega/m$ for the case of an 8 cm wide strap with side slots extending 1 cm behind the strap. The results are shown in Figs. 4a and 4b. It can be seen that increases in strap width have a relatively small effect on the magnitude of the peak tuning loop voltage, while increasing the slot length has a larger effect, due to its effect on R which the VSWR is relatively sensitive to. On the other hand, increasing the strap width does significantly decrease the maximum strap voltage, while increasing the slot length has relatively little effect. Since minimizing the voltage in both regions is desirable, the antenna can be optimized with respect to both parameters by using a wide current strap and making the side slots as long as possible.

In the C-Mod design the 8 cm strap width was chosen to allow a 2.5 cm toroidal gap between the current strap and the Faraday shield tubes, which are not magnetically insulated from one another in this direction. The 1 cm extent of the slots behind the current strap was chosen for mechanical reasons, but the possibility of extending them further is under examination. It is important to point out however, that even without further optimization, the calculated maximum voltages of 28 kV on the current strap and 50 kV in the resonant loop for 2 MW of input power are within an acceptable range. Comparable voltages have been achieved on ICRF antennas currently in use on the Tokamak Fusion Test Reactor (TFTR)⁸. A mockup following the actual antenna geometry will be built in the near future in order to obtain more accurate values of the current strap transmission line parameters.

Tuning/Matching System

A simplified schematic of the antenna circuit is shown in Fig. 7. The two ends of the current strap are fed by an external section of transmission line forming a loop. There are two short shunt lines terminated in capacitances and located near the feed point of the loop. The capacitors to be used in the actual circuit are Comet CV7W units having a capacitance range of 15-150 pF, a peak working voltage of 55 kV, and a current limit of ~ 850 A in continuous operation at 80 MHz.

The capacitances required for a match at the feed point can be determined as follows: Using a simple impedance transformation and assuming ideal lines (except for the current strap), the susceptances looking into both legs at the tee are given by the expression

$$B_{iT} = -\frac{1}{Z_0 \tan(\beta l_i)} \pm \sqrt{\frac{G_{iT}/Z_0^2}{G_{iC} \sin^2(\beta l_i)} - G_{iT}^2} \quad (1)$$

where B_{iT} is the susceptance looking into leg i at the tee, G_{iC} is the conductance at the capacitor in line i , G_{iT} is the value of the conductance of line i at the tee, Z_0 is the characteristic impedance of the lines between the capacitors and the tee, and l_i is the length of line i between the tee and capacitor i . The value of G_{iC} can be calculated from the strap input impedance if the length of the line between the strap and capacitor is known, so that if all transmission line lengths are specified, all of the quantities on the right hand side of the equation are known except for G_{iT} . The negative root gives the value for the longer line and the positive root gives the value for the shorter line.

In order to match to the feed line at the input to the tee, we require that $B_{2T} = -B_{1T}$ and that $G_{1T} + G_{2T} = 1/Z_{in}$, where Z_{in} is the feed line

characteristic impedance. Using these requirements and equation (1) it is possible obtain the values of G_{1T} , G_{2T} , B_{1T} , and B_{2T} . Alternately we can add the requirement that $G_{2T} = G_{1T}$, which is necessary if the amplitudes of the currents on the two halves of the strap are to be exactly equal at any given distance from the short. In this case if l_1 is given then we can use (1) to calculate l_2 , which tells us the optimum tap point. Once these values have been determined in the manner outlined above, the values B_{iC} of the susceptances on the generator side of the capacitors can easily be determined. The values of the susceptances on the load side can also be determined, and the difference between the two values can be used to determine the capacitances required to obtain a match.

The procedure outlined above has been used to determine matching capacitances for a range of plasma loading conditions. Results shown in Fig. 6 indicate that a wide range of resistive and reactive loads can be matched to with small variations in the matching capacitances. The parameters used in these calculations are given in table 1.

Table 1. Transmission line parameters for capacitance calculations.

<u>line</u>	<u>R</u> (Ω/m)	<u>Z₀</u> (Ω)	<u>v/c</u>	<u>length (m)</u>
current strap	6.20	32	0.54	0.48
1	0	50	1.0	1.20
2	0	50	1.0	0.60
3	0	50	1.0	3.71
4 (cap to tee)	0	50	1.0	0.08

Conclusions

The fast wave ICRF launcher designed by ORNL for use on Alcator C-Mod incorporates many features based on the requirements of next generation large tokamak experiments. One of these features is a disruption support mechanism which can handle large loads while allowing thermal expansion of the antenna frame relative to the port, and installation and removal of the antenna from outside the port. Another feature is a low thermal stress, high transparency Faraday shield design which can be adapted to active cooling. A third feature is the minimization of the use of ceramic supports in the antenna transmission line and the location of ceramic vacuum feedthroughs as far from the plasma as possible. A fourth is the use of an external tuning loop with integral tuning elements, allowing tuning in 2-3 frequency bands and matching to a range of plasma loads at the loop feed point, which can be located well within the location of the shield wall. Considerable effort is being applied to optimize the design to allow operation at power levels up to 2 MW.

References

- ¹R. H. Goulding et al., "ICRF Antenna Designs for CIT and Alcator C-Mod", AIP Conference Proceedings, vol. 190, 1989, pp. 250-253.
- ²S. N. Buckley and P. Agnew, "Radiation-Induced Changes in the Dielectric Properties of Insulating Ceramics at ICRH Frequencies", Journal of Nuclear Materials vol. 155-157, pp. 361-365, 1988.
- ³T. L. Owens, F. W. Baity, and D. J. Hoffman, "ICRF Antenna and Feedthrough Development at the Oak Ridge National Laboratory", AIP Conference Proceedings, vol. 129, 1985, pp. 95-98
- ⁴Y. Takase et al., "Alcator C-Mod ICRF Fast Wave Antenna Design and Analysis and Expected Performance", AIP Conference Proceedings, vol. 190, 1989, pp. 346-349.
- ⁵P. M. Ryan et al., in Proceedings of the 15th European Conference on Controlled Fusion and Plasma Heating, Dubrovnik, 1987, part II, p.795.
- ⁶P. M. Ryan et al., Edge Physics Mtg.
- ⁷P. M. Ryan et al., "Magnetostatic Analysis of ICRH Antenna Structures: Application to the DIII-D RF Coupling Improvements", Bulletin of the American Physical Society, vol 33, 1988, p. 2017.
- ⁸D. J. Hoffman, private communication.

DISCLAIMER

This report was prepared as an account of work sponsored by an agency of the United States Government. Neither the United States Government nor any agency thereof, nor any of their employees, makes any warranty, express or implied, or assumes any legal liability or responsibility for the accuracy, completeness, or usefulness of any information, apparatus, product, or process disclosed, or represents that its use would not infringe privately owned rights. Reference herein to any specific commercial product, process, or service by trade name, trademark, manufacturer, or otherwise does not necessarily constitute or imply its endorsement, recommendation, or favoring by the United States Government or any agency thereof. The views and opinions of authors expressed herein do not necessarily state or reflect those of the United States Government or any agency thereof.

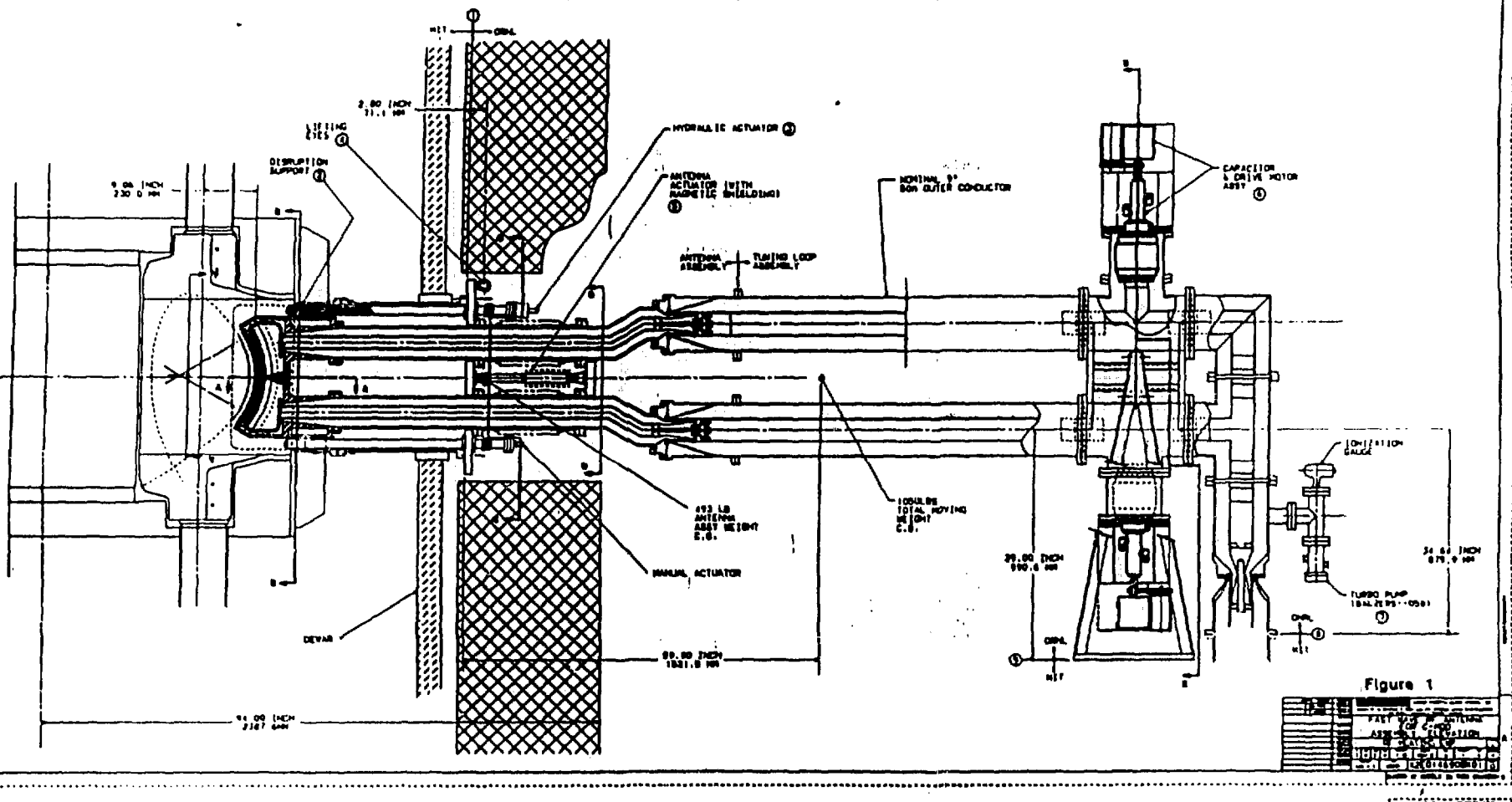


Fig. 1. The ORNL antenna for Alcator C-Mod

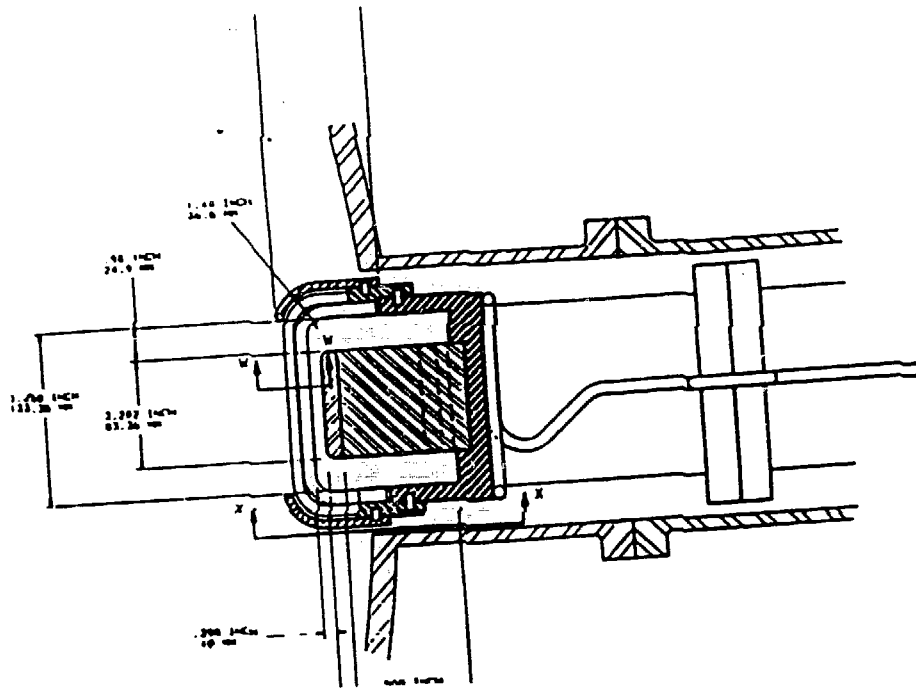


Fig. 2. Top view showing Faraday shield tubes

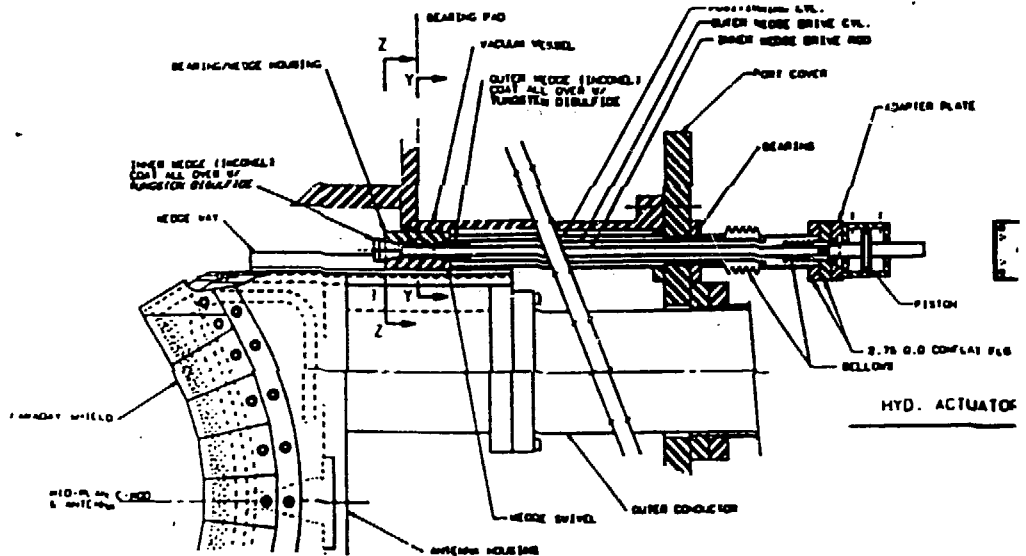


Fig. 3. Disruption support mechanism

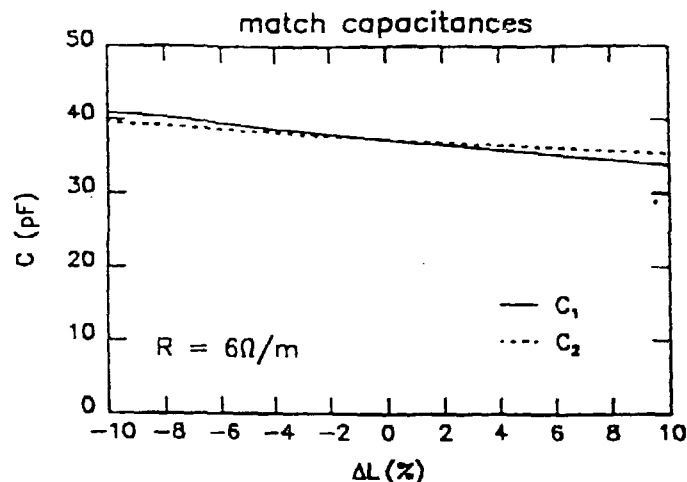
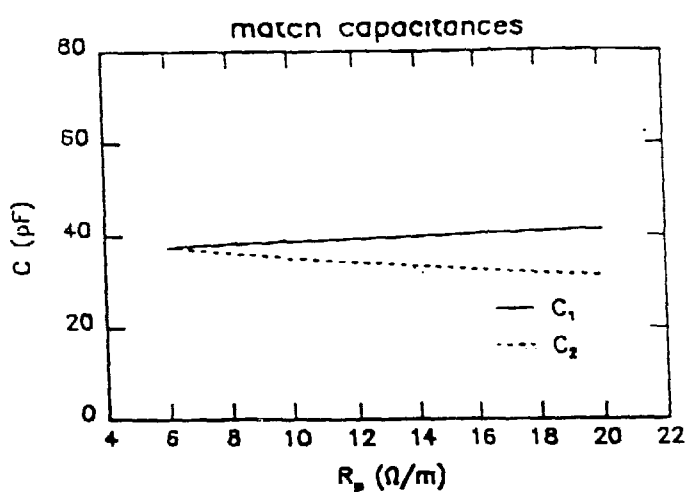


Fig. 6. a) Variation of matching capacitances with changes in resistive loading
 b) Variation of matching capacitances with changes in reactive loading

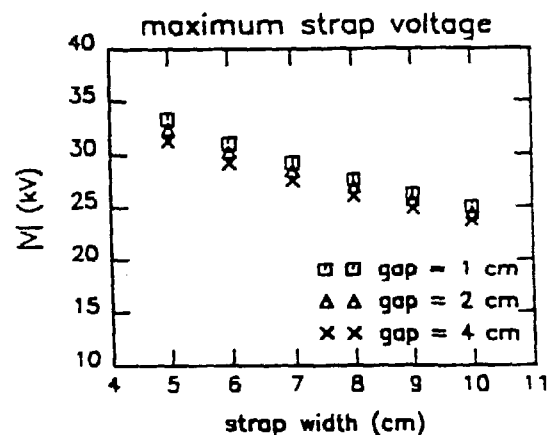
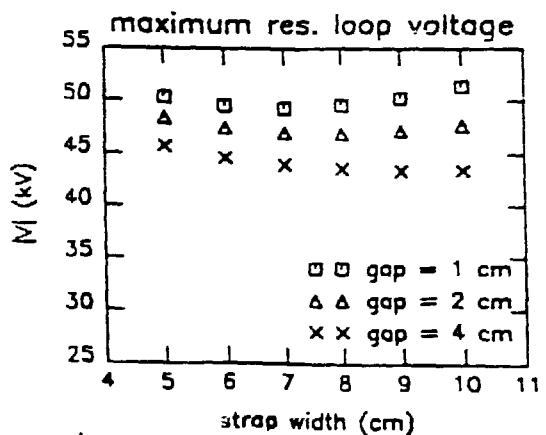


Fig. 4. a) Effect of changes in current strap width and distance that slot extends behind strap on peak resonant loop voltage. b) Effect of these changes on peak voltage on the current strap

Transmission line circuit model

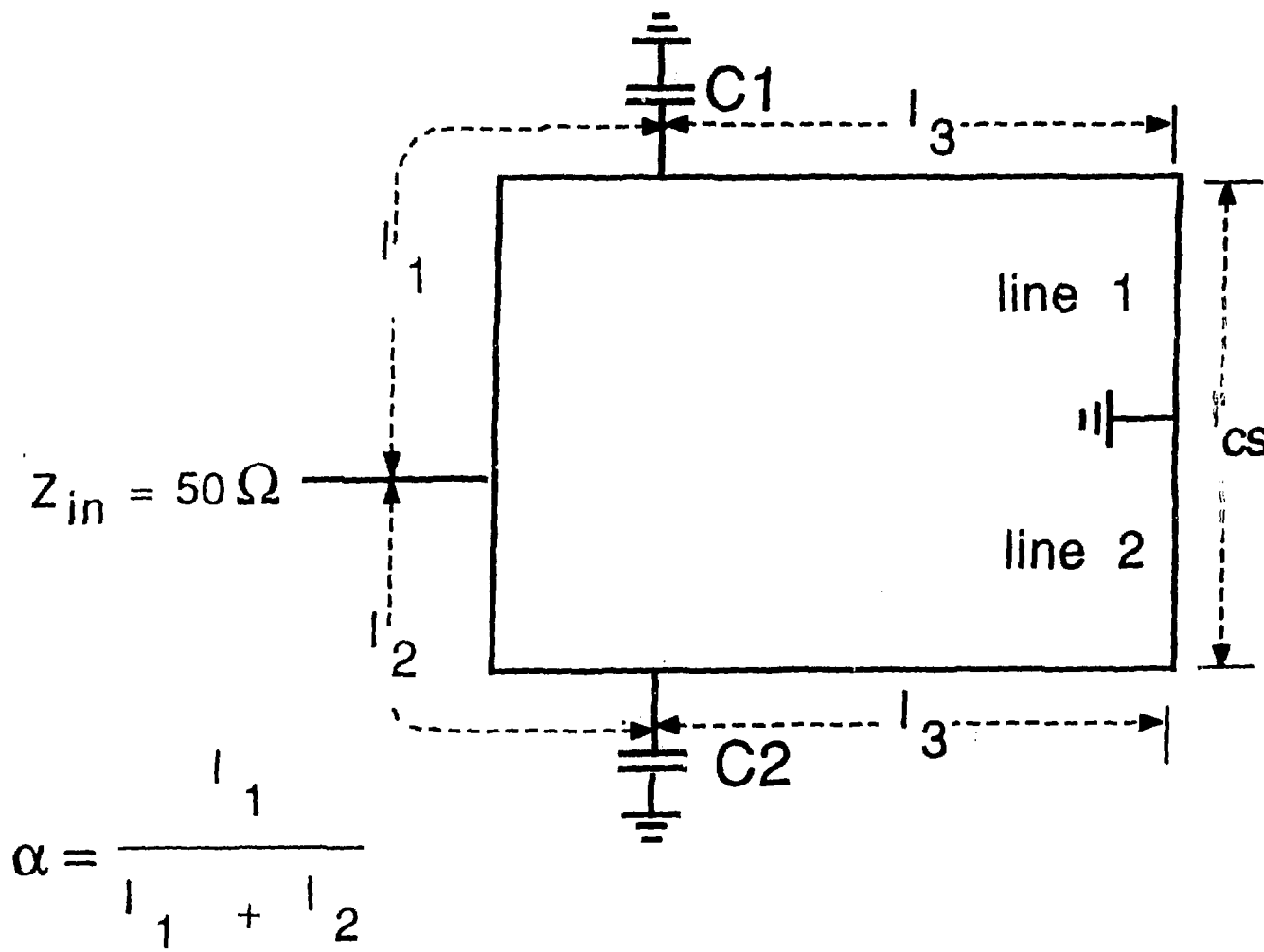


Fig. 5. Schematic of antenna/tuning loop circuit